Available on CMS information server

CMS AN -2010/157

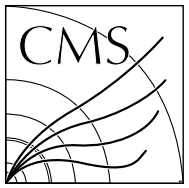

The Compact Muon Solenoid Experiment

Analysis Note

The content of this note is intended for CMS internal use and distribution only

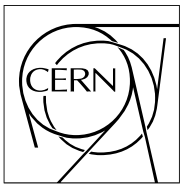

03 June 2010 (v6, 14 July 2010)

α_{T} and its H_{T} Dependence in 7 TeV Data

Paul Geffert and David Stuart
University of California, Santa Barbara

Abstract

We present a study of the correlation of the QCD background rejection power of α_{T}, a potentially useful variable for rejecting QCD in hadronic SUSY searches, with H_{T} in $57\ \mathrm{nb}^{-1}$ of pp collisions at $\sqrt{s} = 7$ TeV. We find that QCD rejection using α_{T} improves with increasing H_{T}, for the H_{T} region explored. Using data driven methods to explore various causes of α_{T} failure, we find that the variable continues to fail less often with increasing H_{T}.

1 Introduction

In some regions of supersymmetry (SUSY) parameter space squarks can be pair produced and decay directly to a quark and lightest supersymmetric particle (LSP) [1], i.e. $\tilde{q} \to q + \tilde{\chi}^0$. Events of this type would produce a dijet signature due to the two quark jets as well as missing transverse energy ($\not\!\!E_{\rm T}$) due to the two LSPs. Because of its enormous cross section, QCD is a major background to this signal.

$\alpha_{\rm T}$, introduced in [2], is a powerful variable for rejecting backgrounds, especially QCD, in SUSY dijet searches. It is defined as

$$\alpha_{\rm T} = \frac{E_T^{j2}}{M_{T\rm inv}^{j1,j2}}, \tag{1}$$

where the two jets are ordered by descending $E_{\rm T}$ and $M_{T\rm inv}^{j1,j2}$ is the invariant mass of the two jets. Assuming massless jets, we can rewrite this for multi jet events [3] as

$$\alpha_{\rm T} = \frac{1}{2}\frac{H_{\rm T} - \Delta H_{\rm T}}{\sqrt{H_{\rm T}^2 - \not\!\!H_{\rm T}^2}}, \tag{2}$$

where $\vec{\not\!\!H}_{\rm T} = -\sum_i \vec{p}_{\rm T}^{\,j_i}$ and $H_{\rm T} = \sum_i p_{\rm T}^{j_i}$. $\Delta H_{\rm T}$ is found by grouping the jets into two pseudo-jets and taking the minimal value of $|p_{\rm T}^{\rm pseudojet1} - p_{\rm T}^{\rm pseudojet2}|$ over all possible pseudo-jet combinations as the value of $\Delta H_{\rm T}$. To partition of the multi-jet system into two pseudo-jets, we separate the jets into two groups and vectorially sum their transverse momenta.

In well measured QCD dijet events, $\not\!\!H_{\rm T}$ will be small which would give $\alpha_{\rm T} \leq 0.5$. However, due to jet energy and phi resolution effects, we will assume $\alpha_{\rm T} < 0.55$ for well measured QCD events from this point forward. In SUSY events, however, there will be real missing transverse momentum due to the production of LSPs. From Eq. 2 we see that when $\not\!\!H_{\rm T}$ is a significant fraction of $H_{\rm T}$, $\alpha_{\rm T}$ can be significantly greater than 0.5. Therefore, SUSY events can frequently have $\alpha_{\rm T} > 0.55$.

Despite the fact that $\alpha_{\rm T} < 0.55$ for well measured QCD events, it is possible that poorly measured QCD events may be above the $\alpha_{\rm T}$ threshold of 0.55. In the case that a jet in the event is lost or fluctuates below threshold, the resulting $\not\!\!H_{\rm T}$ can be great enough to cause $\alpha_{\rm T}$>0.55. If $\alpha_{\rm T}$ is to be used as a background rejection tool, it will be important to understand how often it fails to reject background events. Because the SUSY signal would occur at high $H_{\rm T}$, understanding how often $\alpha_{\rm T}$ fails in QCD events as a function of $H_{\rm T}$ is very important.

This analysis will use N-jet (N=2,3,4...) QCD events as well as γ + jets (≥ 1 jet) events to study the relationship between $\alpha_{\rm T}$ and $H_{\rm T}$. The QCD sample has a much greater cross section and hence superior statistics, but the γ + jets sample can serve as an important cross check as we expect real photons to be better measured than jets. Note that when we compute $\alpha_{\rm T}$ for a γ + jets event, we simply treat the photon as a jet.

This note is organized as follows: Section 2 describes the event sample and the details of event selection. Section 3 discusses the correlation of $\alpha_{\rm T}$ with $H_{\rm T}$. A simple model relating the likelihood of $\alpha_{\rm T}$ failing to $H_{\rm T}$ can be found in Sec. 4. Sections 5 and 6 compare the behavior of $\alpha_{\rm T}$ for different methods of jet reconstruction and jet $p_{\rm T}$ requirements, respectively. Systematic photon under-measurement in the γ + jets sample is examined in Sec. 7. The note concludes in Sec. 8.

2 Dataset and Event Selection

The datasets used in this analysis consists of the following datasets:

- Jet Data ~ 12 nb^{-1} Integrated Luminosity
  - /MinimumBias/Commissioning10-SD_JetMETTau-v9/RECO
  - /JetMETTau/Run2010A-Jun9thReReco_v1/RECO
- Jet MC
  - /QCD_Pt30-herwigjimmy/Summer09-MC_31X_V3_7TeV-v1/GEN-SIM-RECO
- Photon Data ~ 12 nb^{-1} plus ~ 45 nb^{-1} (**new**) Integrated Luminosity
  - /MinimumBias/Commissioning10-SD_EG-v9/RECO
  - /EG/Run2010A-Jun9thReReco_v1/RECO
  - /EG/Run2010A-PromptReco-v4/RECO ~ 45 nb^{-1} (**new**)

The Commissioning10 data samples are reconstructed in CMSSW 3.5.8 patch3. The Run2010A Jun9thReReco data samples are reconstructed in CMSSW 3.7.0 patch2. The Run2010A PromptReco data sample is reconstructed in CMSSW 3.6.1 patch4. The MC sample is reconstructed in CMSSW 3.5.6. The contents of a subset of the PAT objects are stored in a root tree for offline analysis. Unless noted otherwise, all plots in this note are for data only.

The 45 nb^{-1}/EG/Run2010A-PromptReco-v4/RECO sample is not used in any of the plots in this note until Sec. 7. A small number of event and object selection requirements must be changed in order to include this sample, as discussed in Appendix A. A similar luminosity sample of additional jet data is available but not utilized in this analysis due to a factor of 10 or more prescale on the jet trigger used in this analysis.

The preliminary event selection criteria are:

- Data Only: "Good" run and lumisection as defined by Cert_132440-136119_7TeV_May27thReReco_Collisions10_JSON.txt (June 17, 2010) for the ReReco data Cert_132440-137028_7TeV_StreamExpress_Collisions10_JSON.txt (June 16, 2010) for the non ReReco data.
- Data Only: (BPTX) Trigger L1Bit_TechTrig[0] = true
- Commissioning10 Only: physicsDeclared = true
- Jet Data: HLT_Jet15U = true
- Photon Data: HLT_Photon10_L1R = true
- Data Only: (BPTX) Trigger L1Bit_TechTrig[40||41] = true
- Data Only: (Beam Halo) Trigger L1Bit_TechTrig[36&&37&&38&&39] = false
- (Clean Vertex) Vertex ndof ≥ 5 and $|z| < 15$ cm
- (Reject "Previously known as monster" events) Ntracks ≤ 10 or fraction of tracks with high purity $> 20\%$

Here we use RECO tracks from the collection generalTracks and RECO primary vertices from the collection offlinePrimaryVertices.

This analysis uses PAT calo jets from the collection selectedLayer1JetsAK5 with the following selection criteria:

- $p_T > 40$(15 for $\gamma +$ jets sample) GeV
- $|\eta| < 3$
- Loose JetID
  - EMF> 0.01 (only applied to jets with $|\eta| < 2.6$)
  - fHPD< 0.98 (not in MC)
  - n90Hits> 1 (not in MC)

Here EMF is defined as the Electro-Magnetic Energy Fraction of a jet. fHPD is the fraction of jet energy from the highest energy Hybrid Photo Diode. n90Hits is the number of recHits needed to make up 90% of the jet's energy.

PAT photons are used from the collection cleanLayer1Photons with the following selection criteria:

- $E_T > 15$ GeV
- $|\eta| < 1.4$
- maxEnergyXtal/e3x3< 0.9
- isEBGap = isEEGap = isEBEEGap = 0
- $\sigma_{i\eta i\eta} > 0.002$
- Had/EM< 0.05
- isoEcalDR04$< 4.2 + 0.002 * E_T$
- isoHcalDR04$< 4.0 + 0.001 * E_T$
- isoHollowTrkConeDR04$< 4.0 + 0.001 * E_T$
- PixelSeed = 0

Here the variable maxEnergyXtal/e3x3 compares the ratio of the energy in the highest energy crystal in the super cluster to the energy in the surrounding 3x3 grid and is used for spike rejection. The variables isEBGap, isEEGap, isEBEEGap are flags that signify if the photon cluster lies in or near a gap in the EM calorimeter. $\sigma_{i\eta i\eta}$ is a shower shape variable. isoEcalDR04 (isoHcalDR04) is the sum of the ECAL(HCAL) recHits in a $\Delta R < 0.4$ cone around the photon. isoHollowTrkConeDR04 is the sum of the p_T of tracks within a cone of $\Delta R < 0.4$ around the photon, excluding tracks within a much smaller cone (to ignore conversions). PixelSeed describes whether there is a track seed in the pixels that points to the photon cluster.

For N-jet events, we reject an event if it contains a jet that passes the p_T requirement but fails one of the other requirements. The entire event is rejected in this case because events with one or more jets above p_T threshold that are not included in the H_T or $\not{H}_T$ calculations are much more likely to have large $\not{\alpha}_T$. This removes $\sim$ 2% of N-jet data events that pass all other cuts. Similarly, for $\gamma +$ jets events, we reject an event if it contains a jet or photon above p_T threshold that fails one of the other requirements. This removes $\sim$ 17% of $\gamma +$ jets data events that pass all other requirements.

We only consider central photons because they are much more likely to be well measured than forward photons. One important point is that we ignore jets within a $\Delta R < 0.2$ cone of

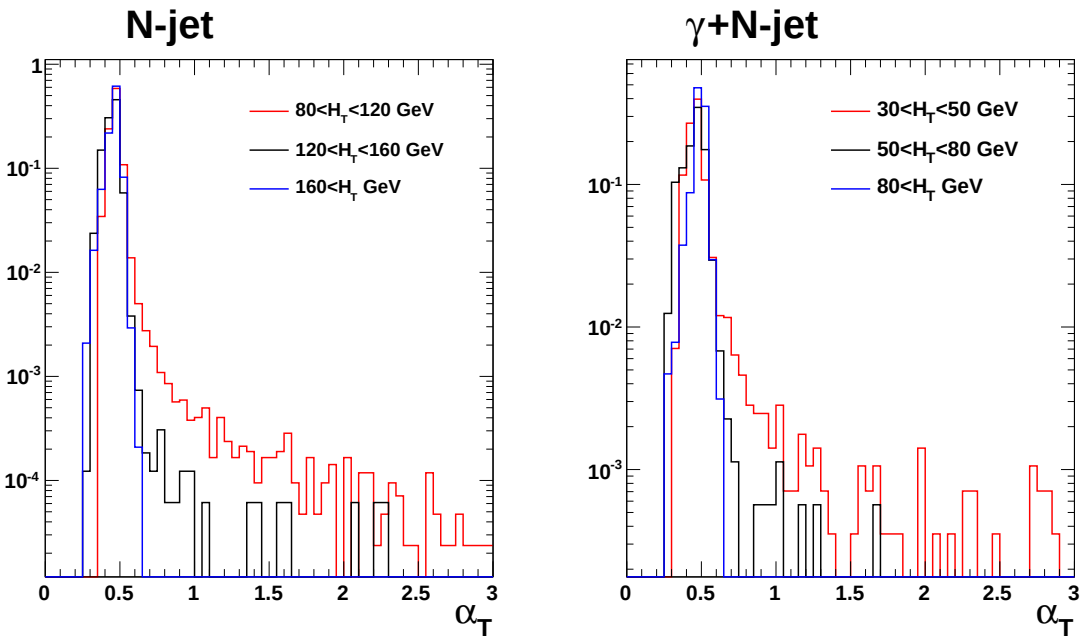

(a) (b)

Figure 1: The α_T distributions for different regions of H_T after all event selection requirements for samples of (a) N-jets and (b) $\gamma +$ jets. Each distribution is normalized to unity for ease of comparison. We can see that the higher H_T distributions have smaller fractions of events with $\alpha_T > 0.55$.

the photon to avoid double counting EM clusters that have been identified as both a photon and a jet. The vast majority of "photons" in our $\gamma +$ jets sample are really jets that fake photons. A key feature of this sample is that the photon energy is systematically under measured compared to the recoiling jets (see Sec. 7 for more details). As we will see in Sec. 3, this has a very significant impact on the α_T variable.

3 Correlation of α_T and H_T

We expect SUSY events to have higher H_T than the average QCD background. This makes it particularly important to understand the behavior of the α_T variable as a function of H_T. The RA1 search [4] includes a data-driven prediction of the QCD contribution at high α_T based on a lower H_T control sample. Here we measure, and study the robustness of, this H_T dependence in first data. In other words, if a dijet or multi-jet search using α_T finds an excess of events at high α_T and H_T, we would like to have confidence that this excess comes from new physics and not our QCD background. As an example of the correlation between H_T and α_T, Fig. 1 shows the α_T distributions after all event selection requirements for different regions of H_T in N-jet and $\gamma +$ jets events. As H_T increases, the α_T distributions have smaller tails above 0.55.

In terms of the definition of α_T in Eq. 2, a substantial difference between 2-jet and $\geq$3-jet events arises due to the use of pseudo-jets to compute ΔH_T in the $\geq$3-jet case. Because ΔH_T is minimized over all pseudo-jet combinations, it has the potential to become much smaller than the $\not{H}_T$ in the event. This is not the case, however, in di-jets, where ΔH_T is fixed (and on the order of the $\not{H}_T$ for back to back dijets). Decreasing ΔH_T for a fixed value of $\not{H}_T$ increases

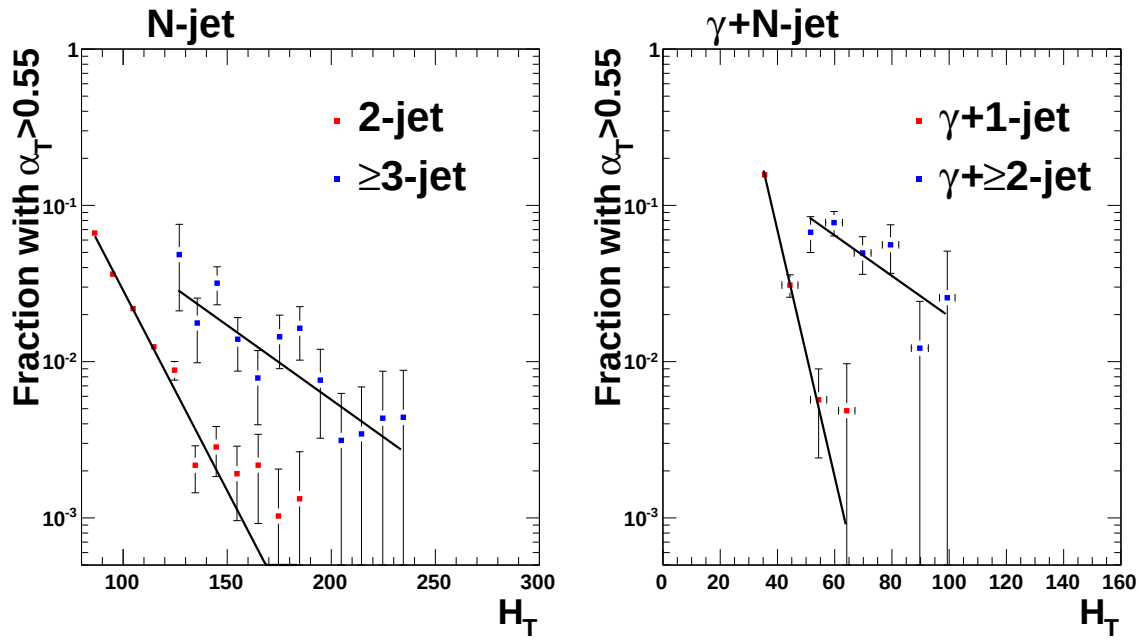

(a) (b)

Figure 2: $f(H_T)$ vs H_T for (a) N-jets and (b) $\gamma +$ jets. The red points are for 2-jet(photon+1-jet) while the blue points are for $\geq$ 3-jet(photon+ $\geq$ 2-jet). In all cases $f(H_T)$ is a decreasing function and consistent with an exponential in the H_T regime shown. Values of H_T below what is shown on each plot are excluded by the selection cuts.

α_T. Based on the above reasoning, we expect α_T to have different behavior in $\geq$3-jet events compared to 2-jet events. Accordingly, almost all of the the plots for the remainder of this note are split into 2-jet(photon+1-jet) and $\geq$3-jet(photon+$\geq$2-jet) samples to investigate this difference.

To help quantify the correlation of α_T and H_T, we introduce a function $f(H_T)$ that represents the fraction of events with $\alpha_T > 0.55$ at a given H_T. By keeping track of the number of events with α_T above and below 0.55 for different H_T bins, we can use our sample to determine the behavior of $f(H_T)$. The results of this are shown in Fig. 2. The red points correspond to a 2-jet(photon+1-jet) sample while the blue points are for a $\geq$3-jet(photon+$\geq$2-jet) sample. In the N-jet samples, for the H_T regime shown, $f(H_T)$ is a decreasing function that is consistent with an exponential. The 2-jet and $\geq$3-jet samples have clearly distinct slopes, as expected. A simple model that may help account for the exponential behavior is described in Sec. 4.

In Fig. 2 there is a much greater difference between the fitted slopes of $f(H_T)$ in the photon+1-jet and photon+$\geq$ 2-jet samples than in the 2-jet and $\geq$ 3-jet samples. This can be explained, at least partially, by the fact that photons are under measured with respect to jets (further described in Sec. 7) in the $\gamma +$ jets samples. Because of the differences in α_T calculations for 2 vs 3 or more object events, we expect the consistent difference in energies of photons and jets to lead to an $f(H_T)$ that falls more quickly for photon+1-jet and less quickly for photon+$\geq$ 2-jet than would be the case if photons and jets had the same energy on average. This is explored further in Sec. 7.

To briefly test the agreement of data and MC, we can compare how the α_T variable behaves in each. Figure 3 shows the $f(H_T)$ distributions of the data and MC N-jet samples. Recall

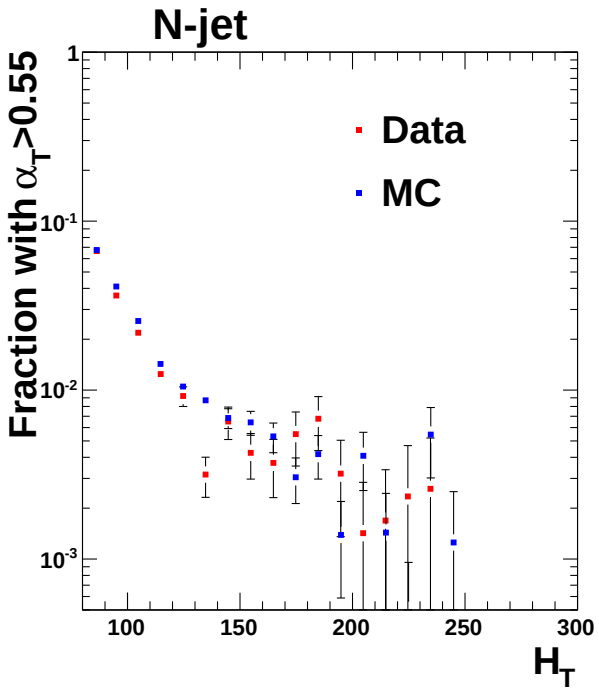

Figure 3: $f(H_T)$ vs H_T for data (red points) vs MC (blue points) N-jet samples. There is reasonable agreement.

that there are slightly different requirements on the data and MC samples, as listed in Sec. 2. The distributions have reasonable agreement.

4 Simple Model for Behavior of $f(H_T)$

4.1 Lost Jets

As mentioned previously, one scenario that can lead to an event failing the α_T cut occurs when there is an additional jet in the event that gets lost. This would occur when an N-jet event loses a jet and the resulting (N-1)-jet event has sufficient $\not{H}_T$ (due to the lost jet) so that α_T falls above 0.55. Taking ΔH_T as zero, we can see from Eq. 2 that the minimum $\not{H}_T$ required to have $\alpha_T > 0.55$ scales linearly with the H_T of the event. If we assume that $\not{H}_T$ is due almost entirely to a lost jet, then as H_T rises the likelihood of losing a high enough p_T jet to fail α_T is highly correlated with the jet p_T spectrum, which is similar to an exponential.

To study these types of events in data, we can utilize an N+1-jet sample and remove jets to obtain an N-jet sample where each event has exactly one missing jet. We can also remove jets from a γ + jets sample for the same effect. Events failing α_T in such a sample will be due to the loss of a jet with overwhelming probability. Figure 4 was produced by removing jets from the N-jet and γ + jets samples, in two different ways, each with linear probability in p_T. Because exponentials dominate lines, the exponential nature of the jet p_T spectrum should be the determining factor that influences $f(H_T)$. For the plots where statistics is great enough, $f(H_T)$ is a decreasing function of H_T and consistent with an exponential. Also, it seems that the $\geq$ 3-jet(photon+$\geq$ 2-jet) samples are less steeply falling than the 2-jet(photon+1jet) samples, consistent with expectations.

The jet removal here is performed with removal probability as a linear function of jet p_T.

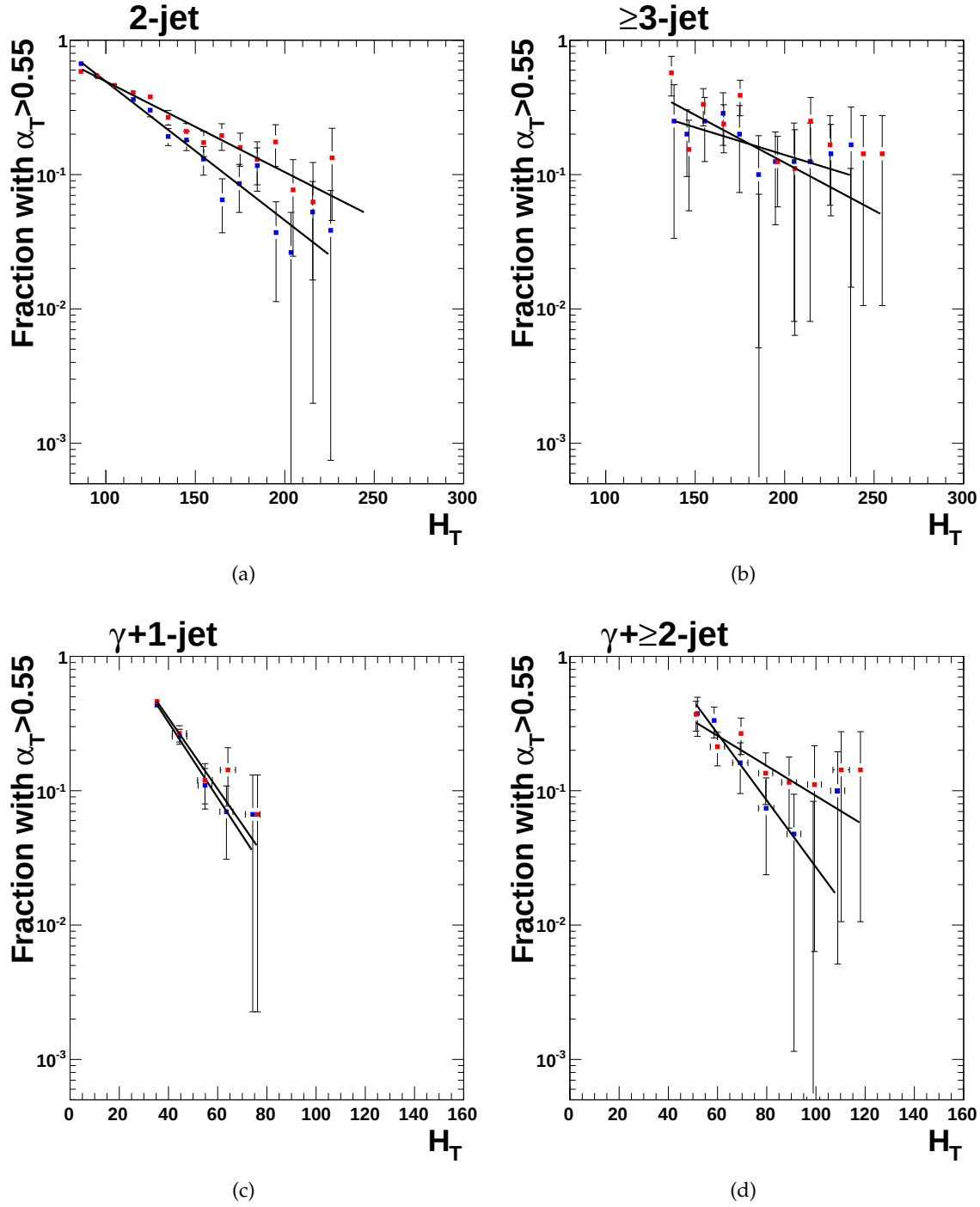

Figure 4: $f(H_T)$ vs H_T for events where exactly one of the jets has been removed resulting in (a) 2-jets, (b) $\geq$ 3-jets, (c) photon+1-jet, and (d) photon+ $\geq$ 2-jets. The sample corresponding to the red data points was obtained by removing 33% of all jets. The sample with blue data points was obtained by removing 50% of jets at p_T threshold with the removal probability linearly decreasing to 0% of 200 GeV and above jets. In these samples, the resulting $f(H_T)$ distributions are decreasing and consistent with exponentials.

This intentionally removes jets from the sample with greater probability than can be reasonably expected in data. For the majority of the p_T range of jets in the sample, the removal probability is at least 5-10 times the probability of jets being smeared below threshold by an asymmetric Gaussian with sigma = 50% of jet p_T applied to 10% of jets. In addition, only events with exactly 1 above threshold jet removed are kept in the sample. Even with this extreme removal of jets, the failure fraction remains a decreasing function of H_T.

One complication of this simple model is that the p_T spectrum of the removed jets will be different for different regions of H_T. As an example, the p_T of the removed jet should be less than the H_T of the remaining jets due to momentum conservation. This effect of a variable p_T spectrum of the removed jets can potentially create additional functional forms for $f(H_T)$, possibly to the extent that $f(H_T)$ is not reliably exponential. It may be possible to study this by varying the way jet removal is performed, once a sufficiently large jet sample is available.

4.2 Soft Jets

Another way that QCD events can have $\alpha_T > 0.55$ is multiple soft jets aligning with similar phi angles. The aligned soft jets create a net momentum in the transverse plane that the remaining jets must balance, giving essentially the same effect as losing a single hard jet. Soft jets will have low p_T and hence will not pass our jet requirements, but will still deposit energy in the calorimeter. This means that the $\not{E}_T$ should account, to some extent, for the soft jets while the $\not{H}_T$ will not. Therefore, events with $\alpha_T > 0.55$ where the $\not{H}_T$ and $\not{E}_T$ are largely uncorrelated in magnitude and/or phi may have failed due to soft jets.

To study these types of events, we create a soft jet enhanced sample by adding soft jets to our usual N-jet sample. There are potentially multiple ways in which this can be done, but we have chosen the following method. Let us assume, for the remainder of this paragraph, that a soft jet with some particular p_T and phi has already been chosen. We first determine the invariant transverse mass of the N-jet system (the H_T) and $\not{H}_T$. Then we create a 4 vector where this invariant transverse mass is given equal and opposite momentum to the soft jet. The resulting boost of this vector is given to the N jets and the H_T and $\not{H}_T$ are recomputed to finish the process. This procedure can be applied iteratively to add as many soft jets as desired.

Using the above method, we can vary the p_T distribution and number of soft jets that are added and observe the effects on $f(H_T)$. We require that a soft jet added to an event be below the jet p_T threshold. In all cases, the soft jets are generated with a distribution random in phi. Figure 5 shows $f(H_T)$ vs H_T for two soft jet enriched samples with different distributions of the number of soft jets and soft jet p_T in N-jet and $\gamma +$ jets samples. The resulting $f(H_T)$ distributions are decreasing functions of H_T. The decrease of $f(H_T)$ as H_T increases makes sense because events with higher H_T should be less affected by adding a soft jet.

4.3 Combined Effects of Lost and Soft Jets

In our sample, there will be events that fail due to a combination of losing a jet and soft jets. Therefore it is important to study the behavior of $f(H_T)$ in a sample that is enriched with both lost jets and soft jets. For completeness, different combinations of jet removal and soft jet addition should be considered. As an example, Fig. 6 shows $f(H_T)$ vs H_T in N-jet and $\gamma +$ jets samples for two such combinations of jet removal and soft jet addition. To produce this plot, we remove exactly one jet from each event in the same way as in Fig. 4 and then add soft jets as in Fig. 5. We can see that $f(H_T)$ is a decreasing function. This result is encouraging

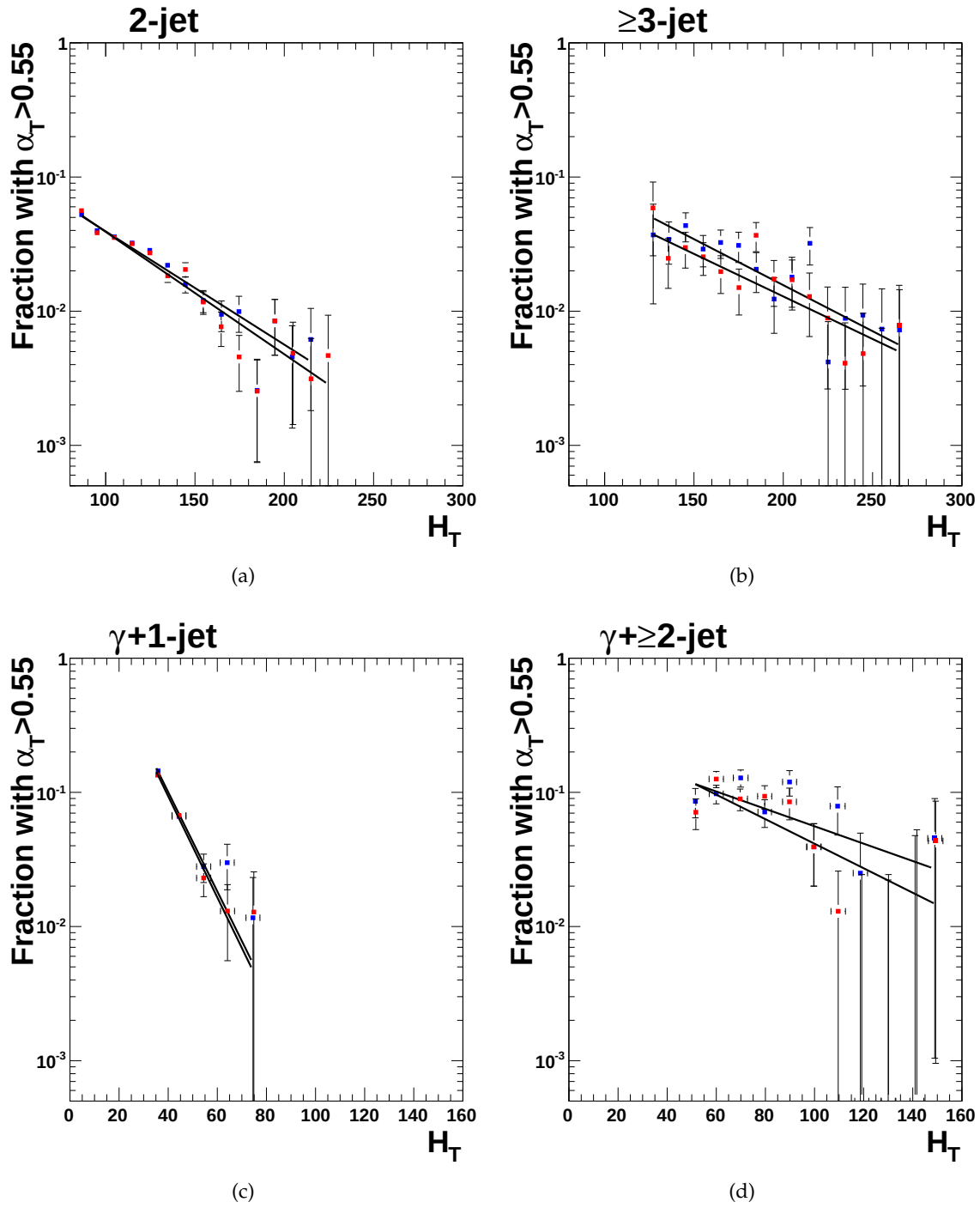

Figure 5: $f(H_T)$ vs H_T for (a) 2-jets, (b) $\geq$ 3-jets, (c) photon+1-jet, and (d) photon+ $\geq$ 2-jets where soft jets have been added. The red points correspond to soft jet addition with the number of soft jets from an exponential distribution with mean 3 and soft jet p_T drawn from an exponential with mean 30(10) for (a) and (b)((c) and (d)). Blue points correspond to soft jet addition with the number of soft jets from an exponential distribution with mean 4 and soft jet p_T drawn from an exponential with mean 20(15) for (a) and (b)((c) and (d)). Note that added soft jets must be below the jet p_T threshold.

because it shows that the samples enriched simultaneously in both lost jets and soft jets that we created still exhibit $f(H_T)$ that decreases with increasing H_T. This helps to demonstrate the robustness of α_T.

4.4 Jet Smearing

A distinct failure mode for α_T is the case where a jet's energy is grossly mis-measured but the jet does not fall below threshold. The mis-measured jet creates a significant amount of $\not{H}_T$ and therefore can have a large effect on the α_T value of the event. Due to the process of minimizing ΔH_T over all pseudo-jets as mentioned earlier, jet mis-measurement can have a distinctly different influence on α_T in 2-jet and $\geq$ 3-jet events. For example, in a back-to-back 2-jet event, a jet mis-measurement will yield $\not{H}_T = \Delta H_T$ thus decreasing α_T below 0.5. However, in a multi-jet event, ΔH_T can be much lower than the $\not{H}_T$ produced by a mis-measured jet and therefore result in $\alpha_T > 0.55$.

Figure 7 shows the results of smearing jets in 2-jet and $\geq$ 3-jet samples separately. The jets are smeared so that large smearing occurs preferentially in the downward direction, which is consistent with jet mis-measurement in data. When smearing jets, it is inevitable that some jets will be smeared below threshold. However, we do not include events with jets smeared below threshold so as to not introduce effects due to lost jets. Therefore, whenever a jet is smeared below threshold, we reset its p_T to its original value and no additional smearing is performed on that jet.

5 Comparison with Different Methods of Jet Reconstruction

One potential topic of interest is how our $f(H_T)$ distribution behaves when using different types of jet reconstruction, i.e. Particle Flow (PF) and Jet Plus Track (JPT). For high enough p_T jets, we expect the differences between the different methods of reconstruction to become less severe. If indeed, the jets in our sample are high enough in p_T for this to be the case, then we might expect the different methods to produce similar α_T distributions.

PAT JPT jets are used from the collection selectedPatJetsAK5JPT. The selection requirements for the JPT jets are identical to the calo-jets, with the one exception that the JPT jets are restricted to $|\eta| < 2.0$, in accordance with the tracker acceptance.

PAT PF jets are used from the collection selectedPatJetsPF with the AK5 algorithm. Unlike the two other classes of jets, PF jets have a distinct set of ID requirements. They are as follows:

- $p_T > 40$ GeV
- $|\eta| < 3$
- neutral hadron fraction < 1.0
- neutral electromagnetic fraction < 1.0
- charged electromagnetic fraction < 1.0
- charged hadron fraction > 0.0 and charged multiplicity > 0.0 (only applied to jets with $|\eta| < 2.4$)

For both the JPT and PF jet samples, events are discarded if they contain a jet that passes the p_T requirement but fails one of the other requirements. This is identical to what is done in the calo-jet sample.

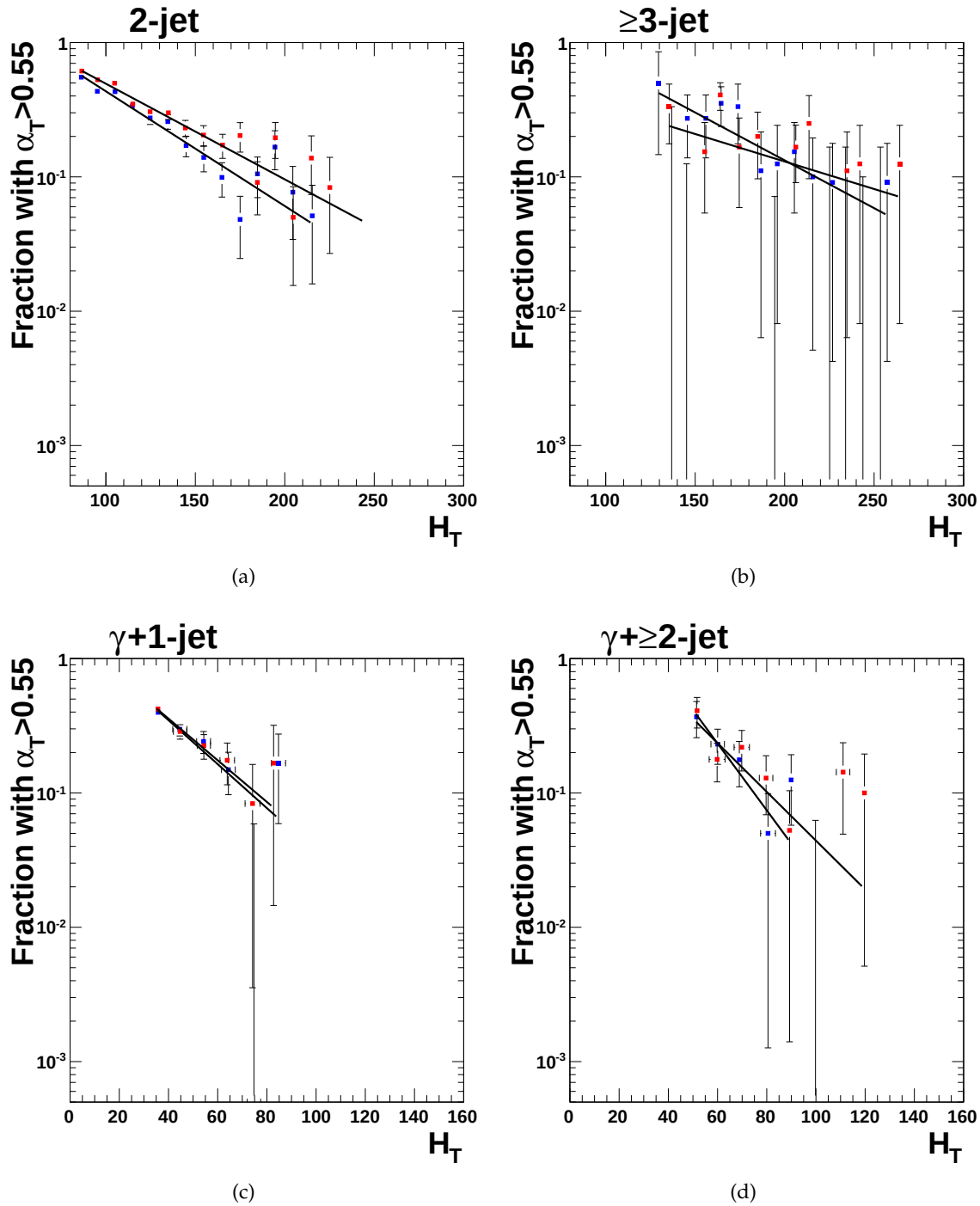

Figure 6: $f(H_T)$ vs H_T for (a) 2-jets, (b) $\geq$ 3-jets, (c) photon+1-jet, and (d) photon+ $\geq$ 2-jets events enriched in both soft jets and lost jets. We remove jets as in Fig. 4 and then add soft jets as in Fig. 5. In all cases, the result is a decreasing function of H_T.

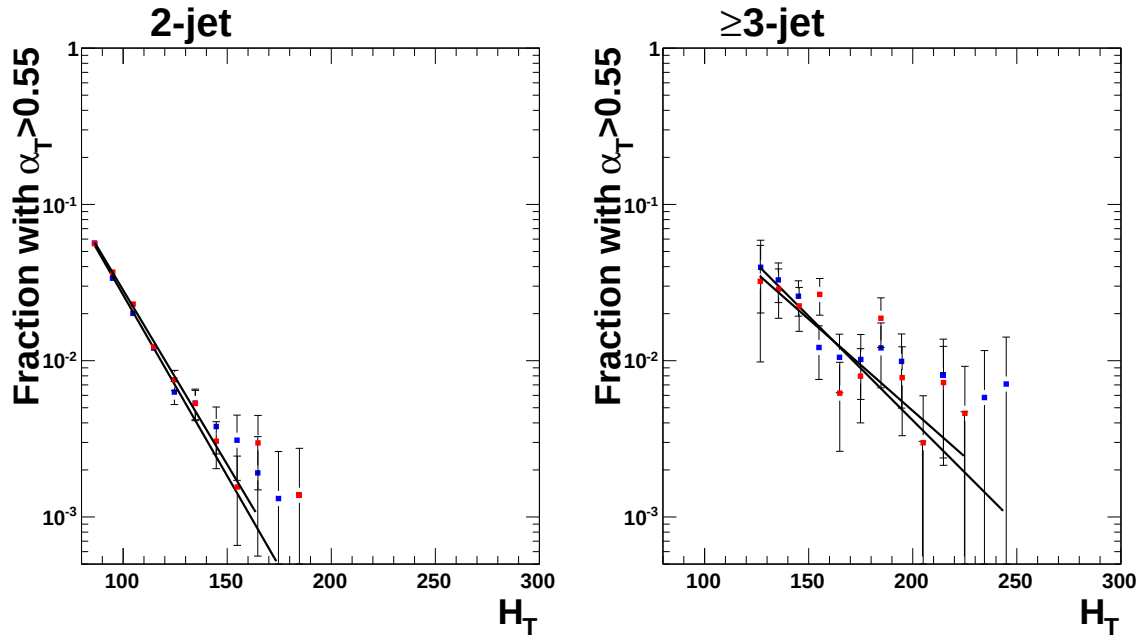

(a) (b)

Figure 7: $f(H_T)$ vs H_T for (a) 2-jets and (b) $\geq$ 3-jets events enriched in smeared jets. The red points have jets smeared symmetrically with a 10% Gaussian 90% of the time and smeared downward with a 50% Gaussian 10% of the time. The blue points have jets smeared symmetrically with a 10% Gaussian 50% of the time and smeared downward with a 50% Gaussian 50% of the time. The resulting samples are fairly similar to the original $f(H_T)$ distributions found in Fig. 2(a).

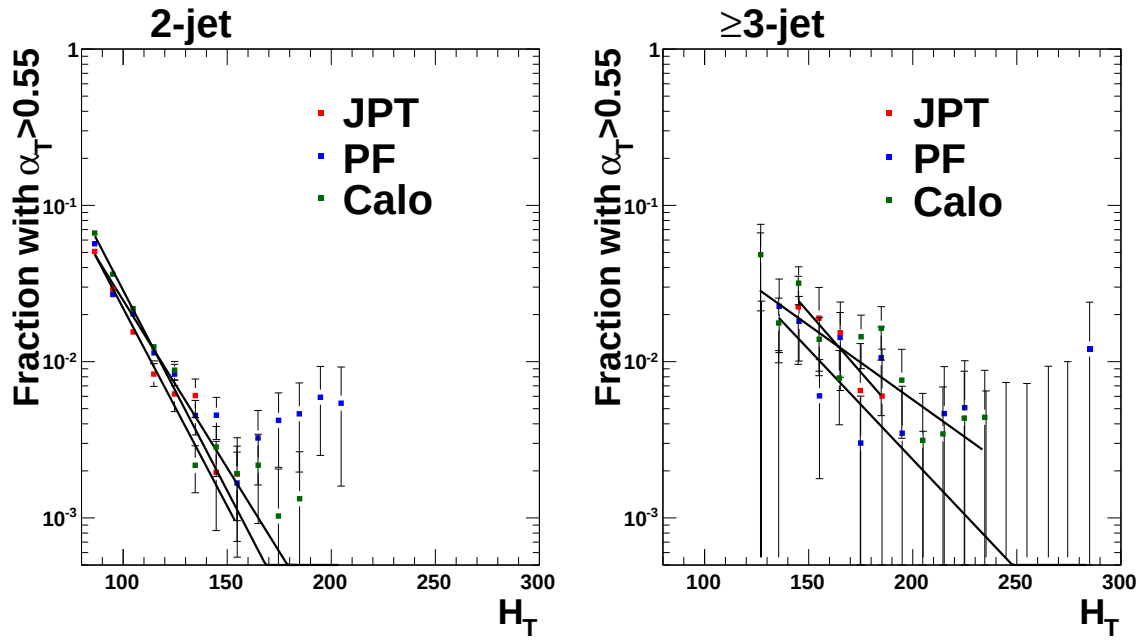

(a) (b)

Figure 8: $f(H_T)$ vs H_T for (a) 2-jets and (b) $\geq$ 3-jets samples for calo, JPT, and PF jets.

Figure 8 shows $f(H_T)$ in our N-jet sample for calo, JPT, and PF jets. JPT and calo jets seem to behave similarly, despite the much more restrictive η requirement on JPT jets. The biggest discrepancy is the high H_T behavior of the PF jets. In the two jet case, the PF jets exhibit similar behavior to the other types until $H_T \sim 150$ GeV, at which point $f(H_T)$ begins to flatten or possibly increase with H_T.

We have examined each of the 6 highest H_T events with $\alpha_T > 0.55$ in the PF 2-jet sample and compared them to the same events in the calo-jet sample. In one of these events, both the PF and calo jet collections have exactly two jets above threshold. The PF and calo jets in this event match fairly well, but there is just enough difference so that the PF jets have α_T of around 0.56 and the calo jets have α_T of around 0.54. However, in the other 5 events, there are exactly 2 PF jets above threshold and 3 calo jets above threshold. In each event, the extra jet in the calo jet collection is nearly the same as the $\vec{\not{H}}_T$ in the PF jets. So for some reason, the PF jet collection in each these events is missing a high p_T jet, which causes the event to have $\alpha_T > 0.55$.

6 Comparison with Higher p_T Requirements

Another interesting comparison that can be made is to examine $f(H_T)$ for different minimum jet p_T requirements. This is done in Fig. 9 for minimum jet p_T requirements of 40, 50 and 60 GeV for the 2-jet case. The $\geq$ 3-jet case is not shown because it does not provide a useful comparison due to limited statistics in the 50 and 60 GeV samples. For each p_T requirement, $f(H_T)$ remains a decreasing function and consistent with an exponential. However, $f(H_T)$ gets shifted higher as the jet p_T requirement is increased. A higher jet p_T cut will cause otherwise good jets to fall below threshold thus becoming "lost" jets likely to contribute to α_T failure as described in Sec. 4.1. This could account for the upward shift in $f(H_T)$ with

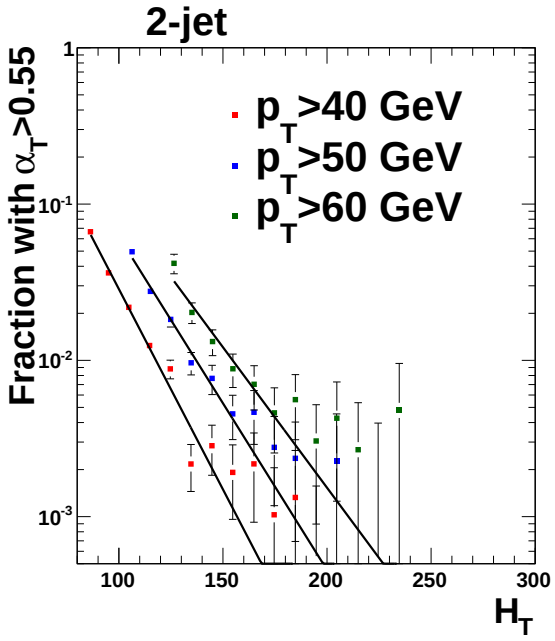

Figure 9: $f(H_T)$ vs H_T for 2-jets samples with various minimum jet p_T requirements. In all cases $f(H_T)$ is a decreasing function and consistent with a falling exponential.

increasing p_T requirement.

7 Photon Energy Under-Measurement

As mentioned previously, the vast majority of "photons" in our $\gamma +$ jets sample are really a jet, generally with an EM fraction close to 1, faking a photon. Due to the nature of photon reconstruction, it is likely that the energy of such a jet that fakes a photon will be greater than the energy of the reconstructed fake photon. This is because the photon reconstruction does not use the HCAL energy of the jet and potentially uses only a subset of the ECAL crystals in which the jet deposited energy.

Some of the difference in E_T between the jet and the photon that it faked should show up in the photon isolation variables isoEcalDR04 and isoHcalDR04, which give the transverse energy of deposits in a $\Delta R < 0.4$ cone around the photon in the ECAL and HCAL, respectively. We can test this by examining the ratio of photon p_T to recoiling jet p_T (not the jet that faked the photon) in pho+1-jet events. Figure 10 shows this ratio before and after adding the isolation energy to the photon's p_T. We can see that without including the isolation energy, the photons are consistently lower p_T than the recoiling jet. After including the isolation energy in the photon's p_T, the average ratio shifts closer to 1. However, both the ECAL and HCAL isolation variables have excluded regions, such as an inner cone, which means we shouldn't expect the isolation energy to completely account for the difference in E_T between the jet and the photon that it faked. Note that all plots in this section use the usual 12 nb^{-1} plus 14 nb^{-1} from the /EG/Run2010A-PromptReco-v4/RECO dataset for a combined 26 nb^{-1} sample. The few changes in selection criteria that are necessary to include the additional 14 nb^{-1} are described in Appendix A.

In Sec. 3, we explained why the systematic under-measurement of photons decreases the

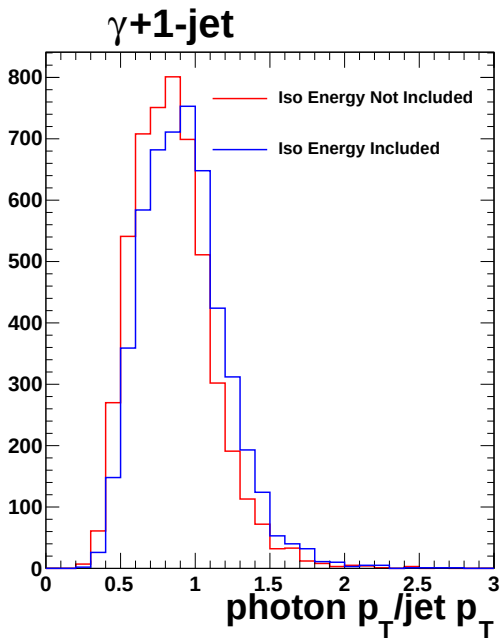

Figure 10: Ratio of photon p_{T} to recoiling jet p_{T} (not the jet that faked the photon) in pho+1-jet events. This is shown with and without including the isolation energy in the photon's p_{T}.

number of events with $\not\!\!\alpha_{\mathrm{T}} > 0.55$ in the pho+1-jet case and increases the number of events with $\not\!\!\alpha_{\mathrm{T}} > 0.55$ in the pho+ $\geq$ 2-jet case. Therefore, by adding the isolation energy to the photon E_{T} in order to remove a large part of this systematic under-measurement, we expect the number of events with $\not\!\!\alpha_{\mathrm{T}} > 0.55$ in the pho+1-jet case to increase and the number of events with $\not\!\!\alpha_{\mathrm{T}} > 0.55$ in the pho+ $\geq$ 2-jet case to decrease. Figure 11 shows $f(H_{\mathrm{T}})$ with and without including the isolation energy for both the pho+1-jet and pho+ $\geq$ 2-jet cases. The results are as expected.

8 Conclusions

We have presented a study of the relationship between the failure of $\not\!\!\alpha_{\mathrm{T}}$ and H_{T} in exclusive N-jet as well as $\gamma +$ jets events and found that $f(H_{\mathrm{T}})$ is a decreasing function of H_{T} in the H_{T} regime studied. We have developed methods to intentionally degrade the data by enriching events with lost jets and/or soft jets as well as smearing jet energies so their effects on $f(H_{\mathrm{T}})$ can be studied. In doing so, we have demonstrated that $f(H_{\mathrm{T}})$ remains a decreasing function for different combinations of these effects. It is interesting that the failure fraction seems to decrease as an exponential, but that is not of central importance. The work contained in this note is summarized in Fig. 12 which shows $f(H_{\mathrm{T}})$ for N-jets, $\gamma +$ jets, N-jets with the removal of jets and addition of soft jets, and N-jets with jet smearing. This figure includes the full 57 nb^{-1} $\gamma +$ jets sample. In the future it may be possible to use Z+jet events as an additional handle on $\not\!\!\alpha_{\mathrm{T}}$, which has been studied in MC [5], to complement this work.

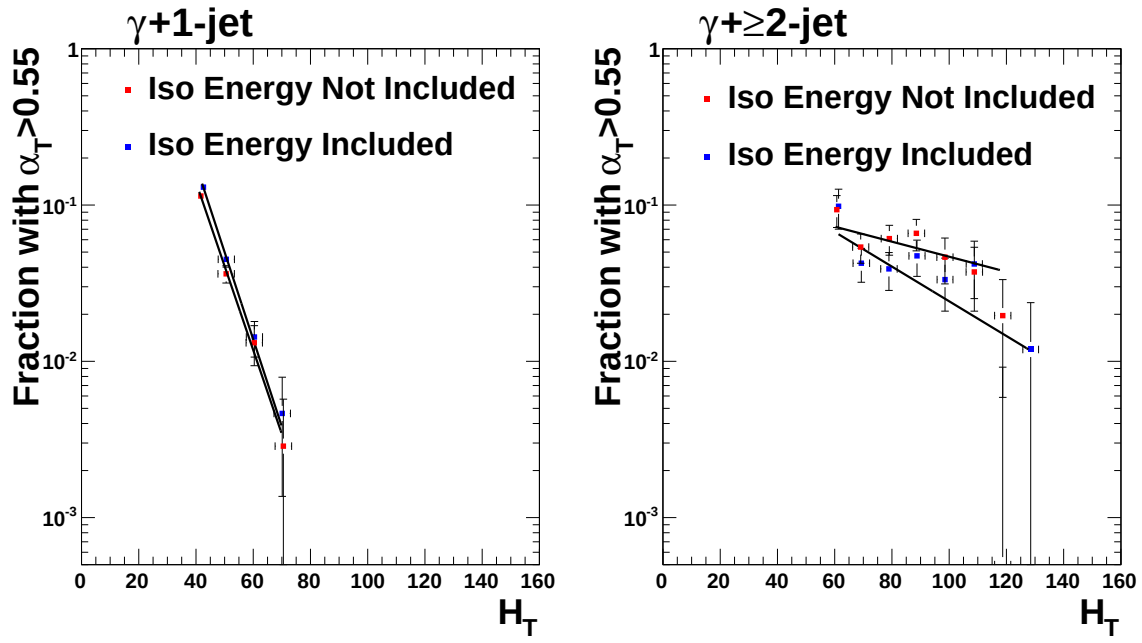

(a) (b)

Figure 11: $f(H_T)$ vs H_T for (a) photon+1-jet and (b) photon+ $\geq$ 2-jet. The red points represent the sample without including the isolation energy of the photon in is p_T. The blue points represent the sample where the isolation energy of the photon is included in is p_T. As described in the text, the behavior of $f(H_T)$ is as expected.

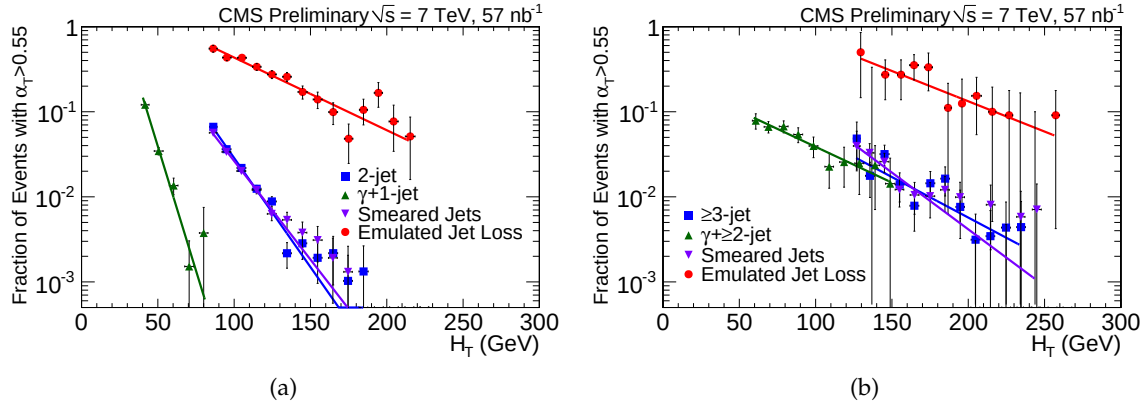

(a) (b)

Figure 12: This figure summarizes the work done in this note by showing $f(H_T)$ vs H_T for various samples. (a) shows 2-jet(pho+1-jet) and (b) shows $\geq$3-jet(pho+ $\geq$ 2-jet). The dark blue points correspond to the usual N-jet sample. The green points are from the full 57 nb^{-1} γ + jets sample. The red points in this plot are from the N-jet sample enriched in both lost jets and soft jets and correspond to the blue points in Fig. 6(a) and (b). The purple points are from the N-jet sample with jet smearing and correspond to the blue points in Fig. 7. In all cases, $f(H_T)$ is a decreasing function.

References

[1] L. Randall and D. Tucker-Smith, "Dijet Searches for Supersymmetry at the LHC," *Phys. Rev. Lett.* **101** (2008) 221803, arXiv:0806.1049.

[2] CMS Analysis Note, CMS-AN 2008/071.

[3] CMS Analysis Note, CMS-AN 2008/114.

[4] CMS Physics Analysis Summary, CMS PAS SUS-08-005.

[5] CMS Analysis Note, CMS-AN 2009/155.

A Additional Data for $\gamma +$ jets sample

Thus far, the $\gamma +$ jets sample in this note has consisted of the samples /MinimumBias/Commissioning10-SD_EG-v9/RECO and /EG/Run2010A-Jun9thReReco_v1/RECO for a total of 12 nb^{-1} integrated luminosity. In this section, we describe the addition of the /EG/Run2010A-PromptReco-v4/RECO sample with 45 nb^{-1} integrated luminosity. However, to include this additional data, we must make a few small changes to our selection criteria.

The differences in selection criteria are necessitated by the implementation of a pre-scale factor in the HLT_Photon10_L1R trigger in the new 45 nb^{-1} of data. To maximize our increase in data, we decide to use the only slightly higher energy trigger HLT_Photon15_L1R. To avoid turn-on effects with the higher energy trigger, we increase our photon E_{T} cut from 15 to 18 GeV. Correspondingly, we increase our jet p_{T} threshold to 18 GeV. Finally, a more up to date good run list, Cert_132440-139790_7TeV_StreamExpress_Collisions10_JSON.txt, is used to filter events. Other than these changes, all of the other requirements described in Sec. 2 remain the same.

Figure 13 shows $f(H_{\text{T}})$ using the above requirements for the 12 nb^{-1}, 45 nb^{-1}, and combined 57 nb^{-1} samples. The reduction of errors allows us to see more clearly that $f(H_{\text{T}})$ decreases in the photon$+ \geq$ 2-jets sample.

Figure 14 is an old version of the summary figure (Fig. 12) where only the original 12 nb^{-1} $\gamma +$ jets sample is shown. Figure 15 is identical except a 26 nb^{-1} $\gamma +$ jets sample is used. This figure was produced with only 14 nb^{-1} from the /EG/Run2010A-PromptReco-v4/RECO sample for an earlier version of this note.

B Fit Parameters

In many of the preceding plots, an exponential fit to $f(H_{\text{T}})$ was performed. This fitting was of the form $\exp(-a \times H_{\text{T}} + b)$, with a and b the fit parameters. Tables 1 and 2 summarize the results of these fits. Figures 12, 14, and 15 are not included because each set of points contained therein is included in an earlier figure in the note.

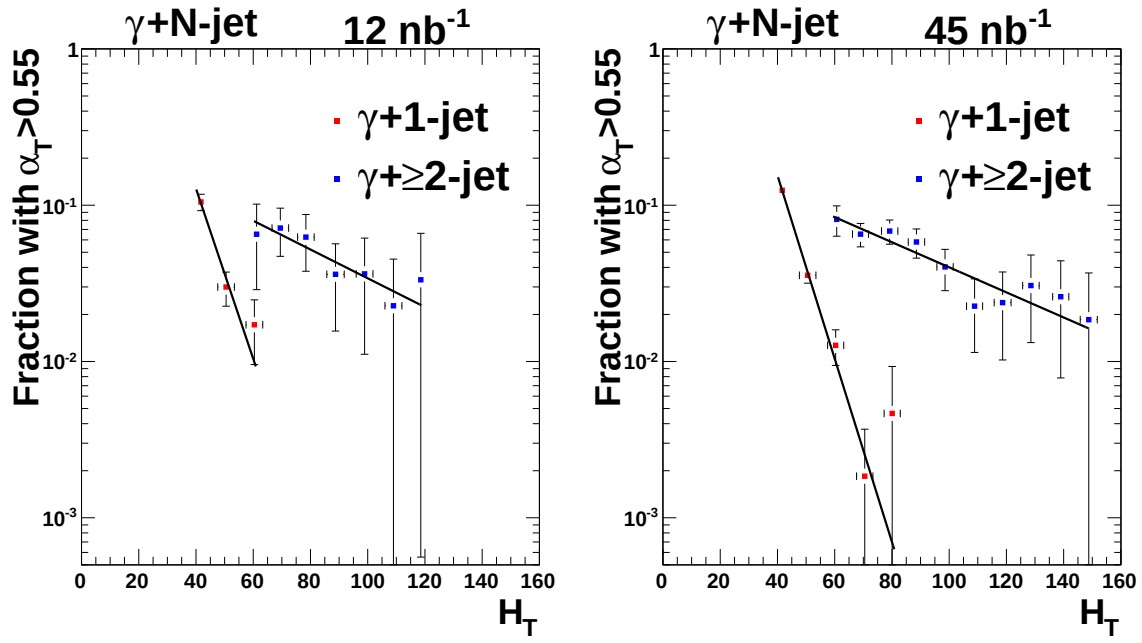

(a)

(b)

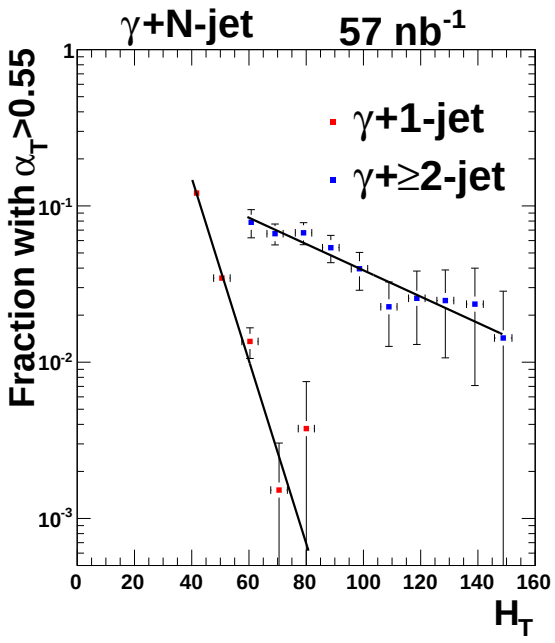

(c)

Figure 13: $f(H_{\mathrm{T}})$ vs H_{T} in γ + jets for the (a) 12 nb^{-1}, (b) 45 nb^{-1}, and (c) combined 57 nb^{-1} data samples. The red points are for photon+1-jet while the blue points are for photon+ $\geq$ 2-jet.

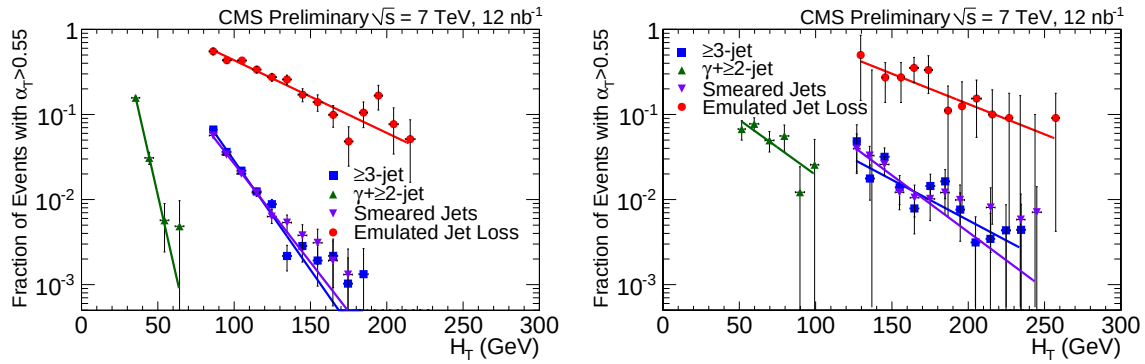

Figure 14: This figure summarizes the work done in this note by showing $f(H_{\mathrm{T}})$ vs H_{T} for various samples. (a) shows 2-jet(pho+1-jet) and (b) shows $\geq$3-jet(pho+ $\geq$ 2-jet). The dark blue points correspond to the usual N-jet sample. The green points are from the original 12 nb^{-1} γ + jets sample. The red points in this plot are from the N-jet sample enriched in both lost jets and soft jets and correspond to the blue points in Fig. 6(a) and (b). The purple points are from the N-jet sample with jet smearing and correspond to the blue points in Fig. 7. In all cases, $f(H_{\mathrm{T}})$ is a decreasing function.

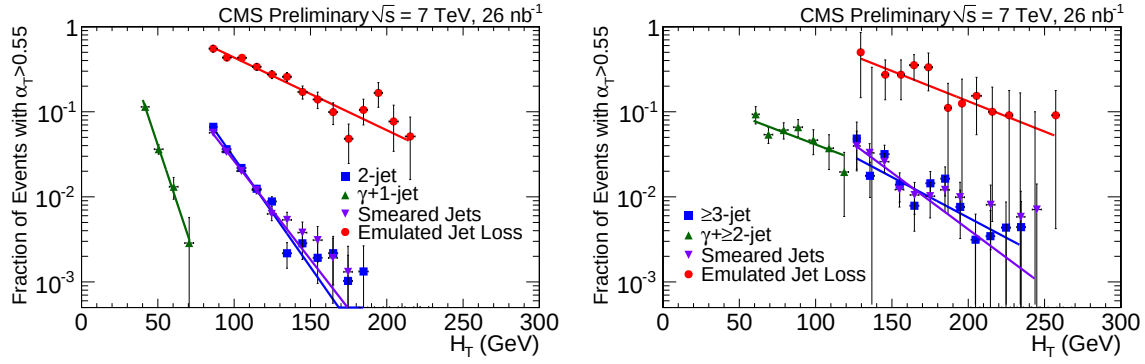

Figure 15: This figure summarizes the work done in this note by showing $f(H_{\mathrm{T}})$ vs H_{T} for various samples. (a) shows 2-jet(pho+1-jet) and (b) shows $\geq$3-jet(pho+ $\geq$ 2-jet). The dark blue points correspond to the usual N-jet sample. The green points are from a 26 nb^{-1} γ + jets sample. The red points in this plot are from the N-jet sample enriched in both lost jets and soft jets and correspond to the blue points in Fig. 6(a) and (b). The purple points are from the N-jet sample with jet smearing and correspond to the blue points in Fig. 7. In all cases, $f(H_{\mathrm{T}})$ is a decreasing function.

Table 1: A list of the fit parameters in the first 6 figures.

Figure	Marker Color	χ^2/Ndof	a	b
2(a)	blue	7.83781/9	-0.02192 ± 0.00661	-0.78077 ± 1.08192
2(a)	red	13.66344/8	-0.05903 ± 0.00239	2.34856 ± 0.23216
2(b)	blue	4.12470/3	-0.02982 ± 0.01018	-0.95620 ± 0.64504
2(b)	red	0.04590/1	-0.18161 ± 0.01742	4.59487 ± 0.64067
4(a)	blue	7.38804/12	-0.02379 ± 0.00140	1.67178 ± 0.15131
4(a)	red	7.56298/13	-0.01554 ± 0.00120	0.84792 ± 0.13454
4(b)	blue	1.41943/8	-0.00942 ± 0.00827	-0.08048 ± 1.44918
4(b)	red	14.82343/10	-0.01635 ± 0.00801	1.17233 ± 1.34992
4(c)	blue	0.30762/2	-0.06459 ± 0.01033	1.45251 ± 0.39987
4(c)	red	1.20886/2	-0.06086 ± 0.01140	1.37703 ± 0.44074
4(d)	blue	0.62628/4	-0.05724 ± 0.01621	2.11114 ± 1.00178
4(d)	red	1.95622/5	-0.02574 ± 0.01177	0.18354 ± 0.78140
5(a)	blue	20.12296/11	-0.01943 ± 0.00109	-1.29124 ± 0.12048
5(a)	red	31.18016/12	-0.02100 ± 0.00112	-1.14277 ± 0.12271
5(b)	blue	9.91082/12	-0.01579 ± 0.00321	-0.99980 ± 0.55808
5(b)	red	9.39218/12	-0.01460 ± 0.00347	-1.42997 ± 0.60251
5(c)	blue	2.55463/2	-0.08521 ± 0.01031	1.11104 ± 0.41187
5(c)	red	0.63500/2	-0.08680 ± 0.00964	1.10258 ± 0.38145
5(d)	blue	16.41223/8	-0.01492 ± 0.00401	-1.39248 ± 0.29428
5(d)	red	18.69011/8	-0.02104 ± 0.00424	-1.07934 ± 0.30129
6(a)	blue	14.43309/11	-0.01966 ± 0.00147	1.13130 ± 0.16930
6(a)	red	11.69584/13	-0.01640 ± 0.00123	0.93457 ± 0.13945
6(b)	blue	4.14463/11	-0.01639 ± 0.00650	1.25936 ± 1.11554
6(b)	red	15.01807/11	-0.00942 ± 0.00701	$-0.15374) \pm 1.24901$
6(c)	blue	3.42734/3	-0.03767 ± 0.00761	0.45129 ± 0.32020
6(c)	red	0.49267/3	-0.03570 ± 0.00850	0.39873 ± 0.35329
6(d)	blue	0.51943/2	-0.05729 ± 0.02089	1.98344 ± 1.25695
6(d)	red	4.64999/5	-0.04181 ± 0.01567	1.06086 ± 0.99379

Table 2: A list of the fit parameters from figure 7 onward.

Figure	Marker Color	χ^2/Ndof	a	b
7(a)	blue	5.72288/7	-0.05334 ± 0.00249	1.69816 ± 0.24064
7(a)	red	1.73385/6	-0.05138 ± 0.00221	1.57280 ± 0.21716
7(b)	blue	6.62873/10	-0.03069 ± 0.00801	0.65514 ± 1.23750
7(b)	red	9.56092/8	-0.02702 ± 0.00834	0.06220 ± 1.33019
8(a)	blue	29.07958/10	-0.04939 ± 0.00304	1.23846 ± 0.30138
8(a)	red	5.41260/5	-0.05829 ± 0.00420	2.01091 ± 0.40797
8(a)	green	13.66344/8	-0.05903 ± 0.00239	2.34856 ± 0.23216
8(b)	blue	5.79725/13	-0.03244 ± 0.01747	0.44194 ± 2.77872
8(b)	red	0.29105/2	-0.03512 ± 0.02997	1.38680 ± 4.71088
8(b)	green	7.83781/9	-0.02192 ± 0.00661	-0.78077 ± 1.08192
9	blue	5.81815/8	-0.04912 ± 0.00411	2.13067 ± 0.49235
9	red	13.66344/8	-0.05903 ± 0.00239	2.34856 ± 0.23216
9	green	6.95497/9	-0.04139 ± 0.00738	1.79794 ± 1.05329
11(a)	blue	0.19682/1	-0.12853 ± 0.01213	3.42998 ± 0.55559
11(a)	red	0.39665/1	-0.12371 ± 0.01268	2.98308 ± 0.56231
11(b)	blue	8.91058/5	-0.02555 ± 0.00879	-1.16482 ± 0.69898
11(b)	red	2.92421/4	-0.01107 ± 0.00756	-1.95649 ± 0.60494
13(a)	blue	0.58733/5	-0.02120 ± 0.01351	-1.25881 ± 1.08477
13(a)	red	1.27069/1	-0.12536 ± 0.02681	2.95635 ± 1.18972
13(b)	blue	2.85324/8	-0.01847 ± 0.00471	-1.36969 ± 0.39211
13(b)	red	1.77748/3	-0.13501 ± 0.01039	3.53714 ± 0.45870
13(c)	blue	2.37803/8	-0.01937 ± 0.00429	-1.31424 ± 0.35568
13(c)	red	3.01768/3	-0.13457 ± 0.00943	3.49033 ± 0.41682